Rapid #: -21171415

CROSS REF ID: **777019**

LENDER: **DAYEHUNIV (Dayeh University) :: Main Library**

BORROWER: **VMC (James Madison University) :: Carrier Library**

TYPE:	Article CC:CCG
JOURNAL TITLE:	Food chemistry
USER JOURNAL TITLE:	Food chemistry.
ARTICLE TITLE:	Identification of alkaline-induced thiolyl-chlorogenic acid conjugates with cysteine and glutathione
ARTICLE AUTHOR:	Druker
VOLUME:	423
ISSUE:	
MONTH:	
YEAR:	2023
PAGES:	136267-
ISSN:	1873-7072
OCLC #:	38873912

Processed by RapidX: 8/24/2023 9:59:18 PM

Food Chemistry 423 (2023) 136267

Contents lists available at ScienceDirect

Food Chemistry

journal homepage: www.elsevier.com/locate/foodchem

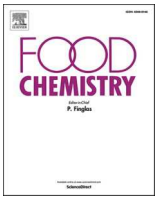

Identification of alkaline-induced thiolyl-chlorogenic acid conjugates with cysteine and glutathione

Charles T. Drucker [a], Amanda R. Cicali [b], Andrew M.P. Roberts [b], Christine A. Hughey [b], Lilian W. Senger [a,*]

[a] Food Science Program, Schmid College of Science and Technology, Chapman University, University Drive, Orange, CA 92866, USA
[b] Department of Chemistry and Biochemistry, James Madison University, 901 Carrier Drive, Harrisonburg, VA 22807, USA

ARTICLE INFO

Keywords:
Chlorogenic acid
Cysteine
Glutathione
LC-MS
Radical conjugation

ABSTRACT

Alkaline reactions of chlorogenic acid (CGA) yield undesirable development of brown or green pigments, limiting the utilization of alkalized CGA-rich foods. Thiols such as cysteine and glutathione mitigate pigment formation through several mechanisms, including redox coupling to reduce CGA quinones, and thiol conjugation, which forms colorless thiolyl-CGA compounds that do not readily participate in color-generating reactions. This work provided evidence of the formation of both aromatic and benzylic thiolyl-CGA conjugate species formed with cysteine and glutathione under alkaline conditions in addition to hydroxylated conjugate species hypothesized to arise from reactions with hydroxyl radicals. Formation of these conjugates proceeds more quickly than CGA dimerization and amine addition reactions mitigating pigment development. Differentiation between aromatic and benzylic conjugates is enabled by characteristic fragmentation of C—S bonds. Acyl migration and hydrolysis of the quinic acid moiety of thiolyl-CGA conjugates yielded a variety of isomeric species also identified through untargeted LC-MS methods.

1. Introduction

Chlorogenic acid (CGA) is a phenolic antioxidant in various foods, beverages, and oilseeds, seeing vast human consumption primarily in coffee beverages (Gigl, Frank, Irmer, & Hofmann, 2022). Retention of CGA's antioxidant activity, which functions to mitigate oxidative stress and modulate metabolic pathways involved in inflammation, is of general interest and utility in CGA-rich food products (N. Liang & Kitts, 2015). Common reactions consuming CGA include the generation of bitter CGA lactones during coffee roasting (Gigl et al., 2022) and the formation of pigments following oxidation by polyphenol oxidase in plants and reactions with proteins, dependent upon the pH of the matrix (Wildermuth, Young, & Were, 2016).

Alkaline processing of food products containing CGA can generate pigmented compounds dependent upon processing conditions and the presence of varying nucleophiles. Alkaline pH can oxidize CGA to an electron-deficient *o*-quinone primed for various potential addition or redox reactions. In the presence of amino acids or proteins, CGA *o*-quinones can produce green, yellow, brown, or colorless compounds depending on the extent of the following four reaction types ordered by decreasing relative rate: thiol addition by a 1,6-Michael reaction, reduction to a catechol via redox exchange, amine addition by a 1,4-Michael reaction or Schiff base formation, and other nucleophilic addition reactions including dimerization (Ito, Sugumaran, & Wakamatsu, 2020). Reactions between oxidized CGA and primary amines in proteins and free amino acids in alkaline beverage and food systems results in the formation of green trihydroxy benzacridine (TBA) derivatives that can limit the commercial viability of chlorogenic acid-

Abbreviations: CA, Caffeic acid (PubChem CID: 689043); CGA, Chlorogenic acid (5-Caffeoylquinic acid, PubChem CID: 1794427); Cys, L-Cysteine (PubChem CID: 5862); Cys-HCl, L-Cysteine hydrochloride (PubChem CID: 60960); DAD, Diode array detector; EIC, extracted ion chromatogram; ESI, electrospray ionization; GSH, L-Glutathione (PubChem CID: 124886); GSSG, Glutathione disulfide (PubChem CID: 65359); HPLC, High performance liquid chromatography; LC-MS, Liquid chromatography – mass spectrometry; Lys, L-Lysine (PubChem CID: 5962); MS^2, tandem mass spectrometry; QqQ MS, triple quadrupole mass spectrometer; TBA, Trihydroxy benzacridine; TWC, total wavelength chromatogram; QA, Quinic acid (PubChem CID: 6508.

* Corresponding author at: Food Science Program, Schmid College of Science and Technology, Chapman University, Keck Center for Science and Engineering, #256 One University Drive, Orange, CA 92866, USA.

E-mail addresses: cdrucker@chapman.edu (C.T. Drucker), cicaliar@dukes.jmu.edu (A.R. Cicali), rob24am@dukes.jmu.edu (A.M.P. Roberts), hugheyca@jmu.edu (C.A. Hughey), were@chapman.edu (L.W. Senger).

https://doi.org/10.1016/j.foodchem.2023.136267
Received 28 January 2023; Received in revised form 16 April 2023; Accepted 26 April 2023
Available online 28 April 2023

containing ingredients (Bongartz, Brandt, Gehrmann, Zimmermann, Schulze-Kaysers, & Schieber, 2016; Iacomino et al., 2017; Namiki, Yabuta, Koizumi, & Yano, 2001; Yabuta, Koizumi, Namiki, Hida, & Namiki, 2001). Mechanistically, TBA compounds are suggested to form by an initial radical-mediated dimerization between two oxidized CGA molecules, followed by subsequent oxidation, amine addition via a 1,4-Michael reaction, and cyclization with loss of water (Bongartz et al., 2016; Namiki et al., 2001). Potential compounds that can mitigate the development of green coloration may do so through participation in thiol conjugation or redox coupling reactions, which are hypothesized to proceed more quickly than the required dimerization and amine addition steps that generate green and brown pigments.

Effective decolorization methods mitigating green compound formation from alkaline CGA-amino acid reactions can facilitate greater consumption of CGA-rich products. The formation of colorless thiolyl-CGA conjugates has been explored to prevent or lessen the extent of green color development in model solutions (Y. D. Liang & Were, 2020; Prigent, Voragen, Li, Visser, van Koningsveld, & Gruppen, 2008) and in alkaline extracted sunflower protein isolates (Ishii, Pacioles, & Were, 2021). Cysteine may prevent greening reactions with CGA primarily through redox regeneration of CGA quinones and secondarily through the formation of cysteinyl-CGA conjugates, which also prevents the loss of antioxidant capacity that can arise from the oxidative consumption of CGA over time (Y. D. Liang & Were, 2020). Furthermore, both cysteine and glutathione delay and limit green color development in a pH-dependent manner, hypothetically arising from differences in thiol pK_a, standard redox potential, and the reactivity of amines proximate to the thiol moiety (Drucker, Senger, & Pacioles, 2023). At pH 8 and 9, GSH resulted in longer lag times before the onset of greening compared to Cys, though Cys resulted in greater mitigation of terminal greening after 48 hr at pH 8 but not at pH 9. However, evidence of the relative rates of redox coupling, thiol conjugation, or other CGA-consuming reactions remains limited, prompting interest in determining reaction products and pathways between competing nucleophiles.

Differences in thiol reactivities at varying pH levels are hypothesized to result in differing greening mitigation characteristics between cysteine and glutathione, which may be optimally utilized depending on processing conditions for CGA-containing foods. Notably, the radical reaction mechanism of thiol conjugation remains debated in the literature, potentially proceeding through homolytic coupling (Kishida, Ito, Sugumaran, Arevalo, Nakanishi, & Kasai, 2021) or through radical coupling (Alfieri et al., 2022), which may yield aromatic or benzylic thiolyl-CGA conjugates (Tošović, Marković, Dimitrić Marković, Mojović, & Milenković, 2017), which are discussed alongside nucleophilic attack through a 1,6-Michael reaction (Ito et al., 2020). The various reaction mechanisms that underlie CGA's antioxidant activity may yield an array of reaction products with mechanisms varying according to pH, such as sequential proton loss electron transfer being preferred over hydrogen atom transfer or radical adduct formation at increased pH (Tošović et al., 2017). Nevertheless, these varied radical and nucleophilic reactions may proceed readily in alkaline solutions, particularly in the presence of thiols such as cysteine, which also readily form thiyl radicals through hydrogen atom transfer (Dénès, Pichowicz, Povie, & Renaud, 2014). Elucidation of the underlying mechanisms and thiol characteristics that govern conjugate formation rates may inform formulation designs or processing approaches to handling chlorogenic acid-rich food exposed to alkaline conditions.

The objective of this work is to describe several thiolyl-CGA reaction products observed in alkaline CGA-lysine-thiol solutions. We hypothesized that a wide array of isomeric conjugate species are generated between CGA and cysteine, and CGA and glutathione, which can be subsequently differentiated based on fragmentation patterns. Identifying these species may shed greater light on the utility of thiols as CGA decolorization agents that maintain antioxidant quality in CGA-rich foods under alkaline conditions.

2. Materials and methods

2.1. Materials and reaction preparation

Chlorogenic acid, L-lysine, anhydrous L-cysteine hydrochloride, and reduced glutathione were purchased from Sigma-Aldrich (St. Louis, MO, USA). Chromatography solvents (LC/MS grade acetonitrile, formic acid) and consumables were purchased from ThermoFisher Scientific (Waltham, MA, USA) and Agilent Technologies (Santa Clara, CA, USA), respectively.

Stock solutions 50 mM CGA, 100 mM Lys, 50 mM Cys, and 50 mM GSH were adjusted to pH 8 and pH 9 using NaOH. Reaction solutions were prepared by mixing solutions in equal ratios to yield solutions of 16.7 mM CGA, 33.3 mM Lys, and 16.7 mM Cys or GSH, with the starting point of the reaction considered upon the addition of the CGA solution. Reaction solutions were incubated at 25 °C for 48 hr in loosely capped vials to allow diffusion of oxygen. Aliquots were taken at 0, 2, 4, 8, 24, and 48 hr and were subjected to LC-MS analysis. Samples awaiting analysis were frozen at −20 °C and thawed before analysis. Samples for the LC-MS were prepared by diluting reaction samples 1:2 in 0.1% formic acid in nanopure water.

2.2. LC-Ms

Agilent 1200 series HPLC instrument (Santa Clara, CA, USA) equipped with a diode array detector (continuous and discrete wavelengths) and a Luna C18(2) column (Phenomenex, Torrance, CA, USA) (150 mm × 4.6 mm inner diameter, 5 μm particle size) was operated at a flow rate of 1.5 mL/min and a column temperature of 25 °C. Mobile phases A (0.1% formic acid in nanopure water) and B (0.1% formic acid in LC-MS-grade acetonitrile) were used in a linear gradient from 5 to 30% B over 13.5 min, with a 3-minute post-run at the initial starting conditions. 10 μL of the sample was injected. Compounds were identified with an Agilent 6460 QqQ MS with a JetStream source operated in positive ion ESI mode (+3000 V, 300 °C, 11 L/min N_2, 35 psi). MS^2 spectra of precursor ions of interest were obtained in product ion scan mode at a rate of 500 ms for m/z 25–1000. Collision energies were compound dependent and ranged from 15 to 25 V.

2.3. Statistical analysis

Alignment and integration of MS data were performed using Agilent MassHunter Qualitative Analysis 10.0 (Santa Clara, CA, USA). Integration data was analyzed using the *xcms* package v. 3.20.0 (Smith, Want, O'Maille, Abagyan, & Siuzdak, 2006) within R v. 4.1.2 (R Core Team, 2022). Compound targeting was performed using principal component analysis, enabling the identification of prospective conjugate species.

3. Results and discussion

3.1. Chlorogenic acid and chlorogenic acid-lysine reaction products

The reaction products and schemes are presented in Fig. 1. Evidence of several CGA dimers was observed with increasing abundances over time in the CGA-only solutions and, to a lesser extent, the CGA-Lys solutions, while the inclusion of thiols resulted in no significant generation of dimeric CGA over 48 hr of incubation (Fig. 2A). Several dimeric isomers of CGA have been reported, though only certain structures proceed to generate green pigmentation upon reaction with Lys (Prigent et al., 2008). Chlorogenic acid dimer compounds with m/z 533.1, arising from hydrolysis of one of the quinic acid (QA) moieties of an intact dimer with m/z 707.2, were the most abundant dimeric species under the alkaline reaction conditions (Fig. 2A). While it is possible that m/z 533.1 compounds may be generated from in-source fragmentation of the dimer, extracted ion chromatograms (EICs) of m/z 533.1 indicate the presence of at least 11 identifiable peaks, some of which do not coincide

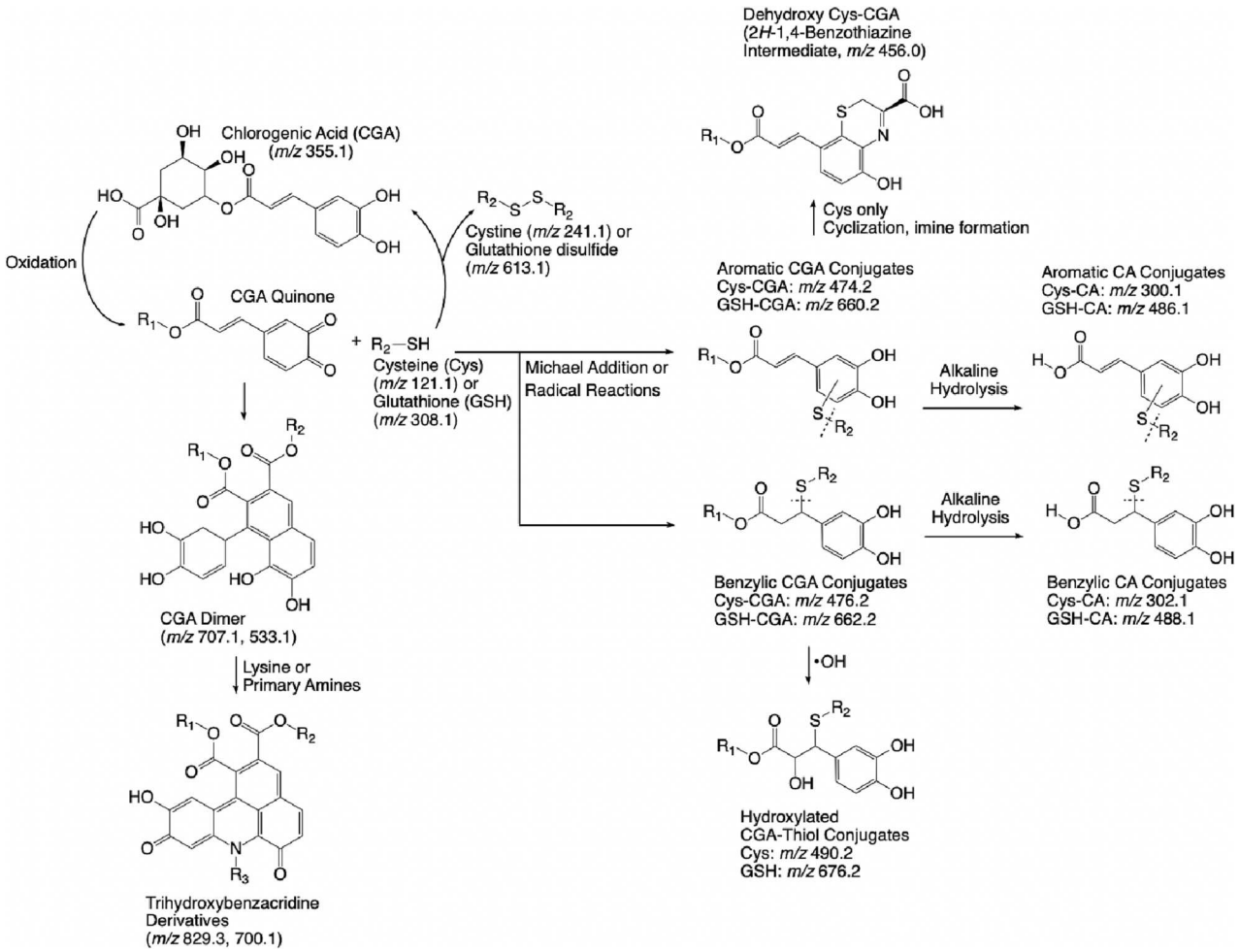

Fig. 1. Proposed reaction pathways involved in chlorogenic acid (CGA) greening and mitigation with cysteine (Cys) and glutathione (GSH), along with proposed reactions involving conjugate species. Mass-to-charge ratio (m/z) values presented correspond to observed masses using positive mode ESI LC-MS, $[M + H]^+$.

with EIC peaks corresponding to the intact dimers of m/z 707.2 (Fig. S1). Thus, the generation of m/z 533.1 may arise from dimerization reactions proceeding in solution involving prior or concomitant loss of the QA moiety. Hydrolytic cleavage of the second QA moiety on CGA dimers, yielding a compound with m/z 341.1, may also proceed in solution or through in-source fragmentation, as these peaks almost exclusively coelute with those of m/z 533.1 (Table 1).

The m/z of 829.2 corresponding to the expected TBA-Lys structure was observed only in CGA-Lys solutions, with greater rates of increase and abundance at pH 9.0 than at pH 8.0 as expected (Fig. 2B, Fig. S2). Solutions containing thiols showed no peaks with this m/z, and correspondingly no green pigmentation. Considering the temporal trends of tentatively-identified CGA dimers, which show nearly zero abundance in solutions containing Cys or GSH over the duration of the experiment, and increasing dimer abundances in CGA and CGA-Lys solutions, it is likely that thiol reactions proceed more readily than both dimerization reactions, reported by Namiki et al. (2001) as the first step in TBA generation, and amine addition reactions.

Only two fragments in the MS/MS data for m/z 829.2 aligned with those reported by Bongartz et al. (2016), though this likely arises from a lower collision energy of 15 eV used in this work. Some of the discrepancies in fragmentation pathways reported herein and those reported by Bongartz et al. (2016) and Schilling et al. (2007) may arise through the specific bond scission that occurs liberating a QA fragment (Table 1). Consistent evidence of in-source fragmentation in this work suggests the formation of an aldehyde upon the liberation of a full QA fragment, while literature tends to report fragmentation of the C—O bond between the ester and the cyclohexane of QA, yielding a carboxylic acid and a dehydroxy QA fragment. Three potentially isomeric structures for TBA species were observed with λ_{max} in the visible range of 515 nm, similar to the values reported by Iacomino et al. (2017) for TBA species in solution with pH between 2 and 3. Three other peaks showed similar absorbance responses at 515 nm, and were associated with m/z values of 847.2 and a coeluting fragment of m/z 655.2, arising from loss of QA. These compounds could be tentatively identified as a hydrated benzacridine derivative, potentially the penultimate intermediate in the reaction scheme proposed by Bongartz et al. (2017). Three peaks with absorbance responses around 460 nm and peaks with m/z 700.1 also align with characteristics of TBA compounds produced through reactions with Lys's α-amine as reported by Iacomino et al. (2017), though these compounds notably formed in higher concentrations at pH 8.0 than at pH 9.0 (Fig. 2C).

3.2. Cysteine-chlorogenic acid reaction products

Aromatic (m/z 474.1, Fig. 3A and S3) and benzylic (m/z 476.1, Fig. 3B) Cys-CGA conjugates were observed based on fragments generated from C—S scission locations analogous to GSH-CGA conjugate fragmentation reported by Xie et al. (2013). Identification of aromatic conjugates was based on fragments indicative of scission of the cysteinyl C—S bond, with a base peak of 195.0 corresponding to losses of QA and a Cys fragment along with fragments of 88.0, 240.0, 282.0, 300.0, and 456.1 in agreement with those reported for 2′-Cys-CGA by Poojary et al. (2023) (Fig. 3A, Table 2). Aromatic Cys-CGA conjugates appeared in the

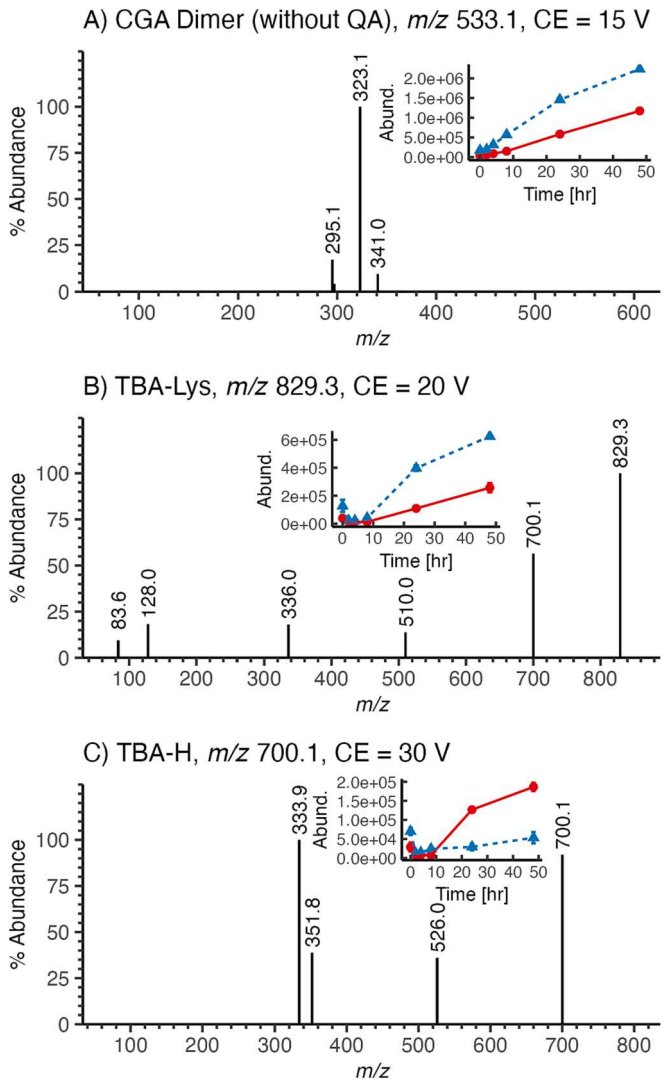

Fig. 2. Fragmentation of (A) chlorogenic acid (CGA) dimer compounds in CGA-only solutions and (B, C) trihydroxy benzacridine (TBA) compounds in CGA-lysine solutions. Inset plots illustrate abundance changes over the 48 hr reaction duration, where the solid red line (—●—) describes solutions at pH 8 and the blue dashed line (- -▲- -) describes solutions at pH 9. In (A), at the collision energy of 15 V, no precursor ion of *m/z* 533.1 remained after fragmentation. (For interpretation of the references to color in this figure legend, the reader is referred to the web version of this article.)

highest abundance during the first measurement, followed by a sharp decrease in abundance over the first 8 hr of incubation. At 24 hr, abundances appeared to increase again, then decrease by 48 hr. The origin of this sporadic increase in conjugate abundances remains undetermined.

Benzylic conjugates included fragments with *m/z* 122.1 and 355.1, indicating fragmentation of the benzylic C—S bond to yield CGA and Cys fragments, in addition to a base peak of 163.1, arising from loss of QA from CGA (Fig. 3B, Table 2). Abundances for the benzylic conjugates were generally ten times higher than those of the aromatic conjugates. Benzylic Cys-CGA conjugates were detected at maximum abundance at the 8- and 4-hour time points for pH 8.0 and 9.0, respectively, with the pH 9.0 solutions showing a steeper decrease in abundance over time compared to pH 8.0. Thus formation of both classes of conjugates appear to proceed extremely quickly within the first hour of incubation, though the relative concentrations of aromatic to benzylic conjugates were not directly measured.

Alkaline hydrolysis of Cys-CGA conjugates yielded aromatic (*m/z* 300.1, Fig. 3C) and benzylic (*m/z* 302.1, Fig. 3D) Cys-CA conjugates. Two significant peaks in the MS spectra were observed during fragmentation of *m/z* 300.1 with different fragmentation patterns. The most abundant *m/z* 300.1 peak at 1.5 min contained a dominant fragment of *m/z* 195.0 in addition to fragments at 88.0 and 240.0, in line with the fragmentation pattern reported for 2′-cysteinyl caffeic acid by Poojary et al. (2023) (Fig. 3D, Table 2). Other peaks at 1.2 min, 1.7 min, and 2.3 min also contained fragments with *m/z* 195.0 at varying intensities, suggesting isomeric products potentially formed through varying regioselectivity of the thiol addition reaction or through cis–trans isomerization of the alkenyl moiety (Fig. S3). Notably, the peak at 1.2 min, the second most abundant of the *m/z* 300.1 peaks, shows a fragment at *m/z* 163.1 approximately 8.5 times more intense than that at 195.0. This peak at 1.2 mins lacks nearly all other fragments characteristic of Cys-CA such that identification of this peak cannot be confidently proposed without a higher mass accuracy instrument.

Two peaks corresponding to *m/z* 302.1 eluted within the first minute of the method, tentatively identified as benzylic Cys-CA conjugates based on evidence of C—S bond scission yielding fragments of 122.0 and 181.1 in the MS^2 spectra (Fig. 3E, Table 2). Three peaks eluting at 1.9, 2.0, and 2.7 min showed similar fragmentation patterns along with other peaks below the signal-to-noise threshold, though the asymmetry of the peak at 2.7 min may be indicative of coeluting compounds. Isomeric forms of benzylic Cys-CA species may occur through cis–trans isomerization of the alkene bond by cysteinyl radicals in solution (Claudino, Johansson, & Jonsson, 2010). Absence of significant formation of caffeic acid arising from hydrolysis of unreacted CGA suggests these conjugates were formed exclusively through hydrolysis of conjugate species, sensibly proceeding more significantly at higher pH.

One predominant hypothesized pathway for decreasing of aromatic Cys-CGA involves dehydration reactions involving conjugates, which may be enabled by the proximity of the cysteinyl α-amine to oxidized quinone oxygens. Three peaks eluting at 6.84-, 8.10-, and 8.28-min containing compounds with *m/z* 456.0 were identified as Cys-CGA reaction products, which also were associated with a bathochromic shift of the CGA absorption peak from 325 nm to approximately 355 nm. This phenomenon may feasibly arise from cyclization of the cysteinyl moiety

Table 1
Precursor ions, fragments, and tentative identifications of compounds observed in chlorogenic acid-only (CGA) and chlorogenic acid-Lysine (CGA-Lys) solutions.

Sample	Precursor	Tentative Identification	Voltage	Fragments
CGA	355	CGA	15	163.1 (100)
CGA	707	CGA Dimer	15	515.1 (100), 497.1 (74), 469.0 (17), 355.2 (16), 354.8 (16), 352.9 (15), 341.1 (26), 323.1 (93), 193.0 (12), 192.5 (12), 162.9 (22)
CGA	533	CGA Dimer without QA	15	341.0 (10), 323.1 (100), 295.1 (17)
CGA	341	CGA Dimer without 2 QA	15	323.0 (99), 297.0 (14), 295.1 (26), 279.1 (11), 249.0 (11), 187.0 (30), 163.1 (100), 162.0 (18), 161.0 (38), 136.0 (25), 135.0 (25), 133.0 (29)
CGA-Lys	829	TBA-Lys	20	829.3 (100), 700.1 (57), 510.0 (14), 336.0 (18), 128.0 (18), 84.1 (9), 83.6 (10)
CGA-Lys	700	TBA-H	30	700.1 (92), 526.0 (36), 525.6 (36), 351.8 (39), 333.9 (100)
CGA-Lys	655	TBA-Lys without QA	20	526.1 (100)

TBA and QA refer to trihydroxy benzacridine and quinic acid respectively.

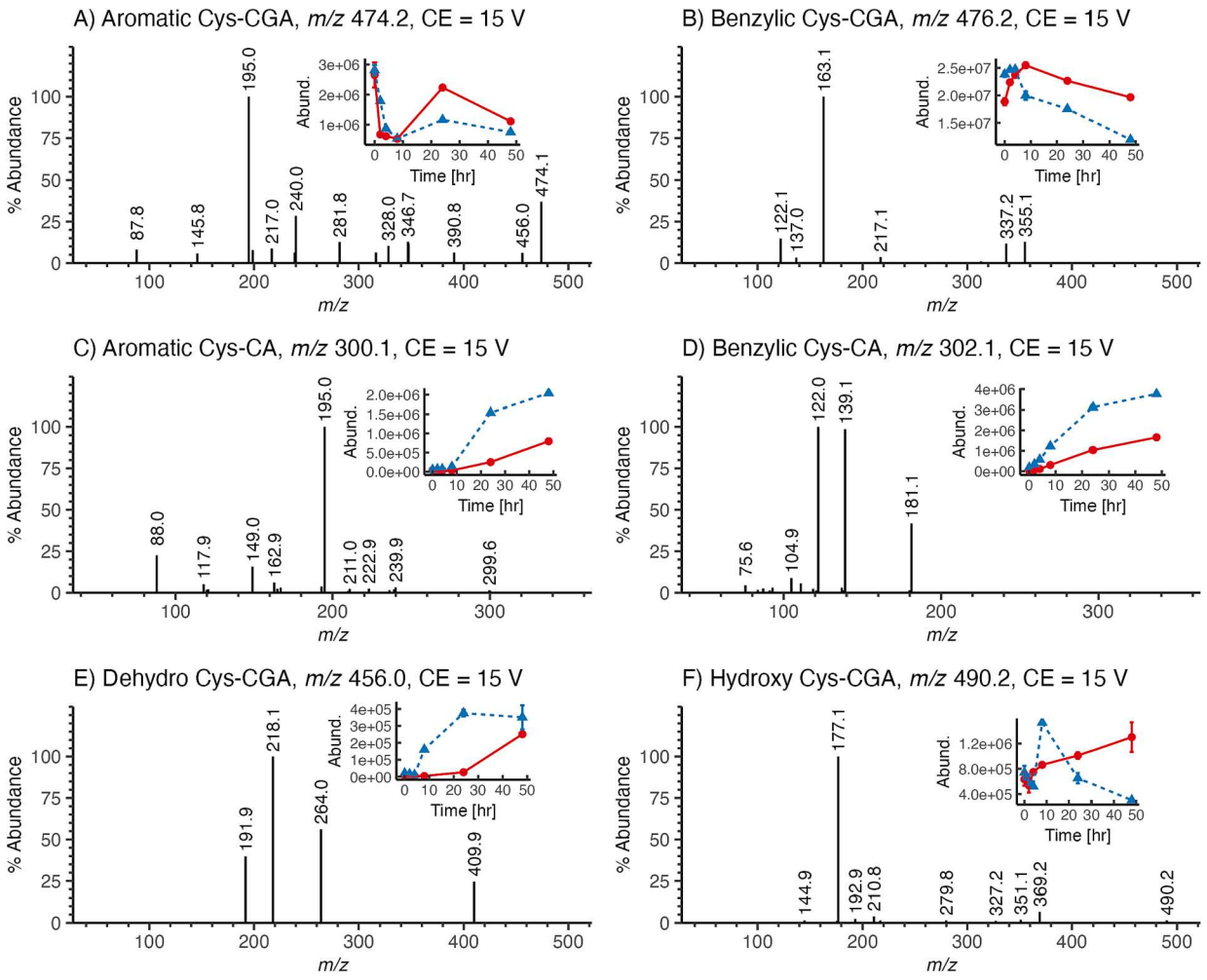

Fig. 3. Fragmentation of conjugates identified in chlorogenic acid-lysine-cysteine solutions. Inset plots illustrate abundance changes over the 48 hr reaction duration, where the solid red line (—●—) describes solutions at pH 8 and the blue dashed line (- -▲- -) describes solutions at pH 9. (For interpretation of the references to color in this figure legend, the reader is referred to the web version of this article.)

Table 2
Precursor ions, fragments, and tentative identifications of compounds observed in chlorogenic acid-lysine-cysteine (Cys) solutions.

Precursor	Tentative Identification	Voltage	Fragments
122	Cysteine	15	105.0 (11), 86.9 (27), 76.0 (100)
300	Aromatic Cys-CA	15	195.0 (100), 162.9 (6), 149.0 (16), 117.9 (5), 88.0 (23)
302	Benzylic Cys-CA	15	181.1 (42), 139.1 (99), 122.0 (100), 110.9 (6), 104.9 (9)
456	Cys-CGA Benzothiazine	25	409.9 (25), 264.0 (56), 218.1 (100), 191.9 (40)
460	Dehydroxy GSH-CGA	15	460.0 (7), 339.0 (6), 147.0 (100)
474	Aromatic Cys-CGA	15	474.1 (37), 390.8 (6), 347.2 (12), 346.7 (13), 328.0 (10), 316.1 (6), 281.8 (13), 240.0 (28), 217.0 (9), 198.8 (8), 195.0 (100), 87.8 (8)
476	Benzylic Cys-CGA	15	355.1 (13), 337.2 (12), 163.1 (100), 122.1 (15)
490	Hydroxy Cys-CGA	15	369.2 (7), 177.1 (100)

CA refers to caffeic acid.

of an aromatic Cys-CGA conjugate to form a 2*H*-1,4-benzothiazine compound (Napolitano, De Lucia, Panzella, & d'Ischia, 2008). Fragmentation of these three compounds yielded fragments with *m/z* 264.0, arising from loss of QA, and 409.9 and 218.1, suggesting losses of a carboxylic acid moiety from the molecular ion and the aforementioned fragment (Fig. 3F, Table 2). Further structural characterization of these species would be required to conclusively identify these species, though the proposed identification may underlie the tendency for alkaline Cys-containing CGA solutions to turn brown over extended incubation (Y. D. Liang & Were, 2020).

Four peaks at 0.9, 1.2, 1.6, and 1.9 min were identified as *m/z* 490.1, with an MS^2 base peak of 177.1 and a second peak at 369.1 (Fig. 3C). These would suggest an original structure of a hydroxylated aromatic Cys-CGA conjugate. These compounds may arise through radical adduct formation between a Cys-CGA conjugate and a hydroxyl radical under aqueous conditions (Tošović & Marković, 2019). At pH 8.0, concentrations of these compounds increased throughout the incubation, while at pH 9.0 a maximum concentration was reached at 8 hr. Hydroxylated CGA compounds have been reported largely as a function of thermal treatment such as during coffee production (Matei, Jaiswal, & Kuhnert, 2012) and through computational methods (Tošović et al., 2019). The experimental results presented here is therefore the first evidence of these reactions proceeding at lower temperatures or with thiolyl-CGA conjugates.

3.3. Glutathione-chlorogenic acid reaction products

Despite poor retention on the C18 column, tracking of GSH (*m/z*

308.1, Fig. S4) based on integration of peaks within the first minute of the method indicated first-order consumption of GSH over time (Fig. 4A), with the rate constant at pH 9.0 approximately 3.4 times higher than at pH 8.0. Formation of glutathione disulfide (GSSG, *m/z* 613.2) proceeded more quickly at pH 9.0, reaching a constant level upon complete consumption of GSH by 48 hr.

Both aromatic (*m/z* 660.2, Fig. 4B and S5A) and benzylic (*m/z* 662.2, Fig. 4C) GSH-CGA conjugates were observed, all of which were identified based on MS^2 fragmentation patterns described by Xie et al. (2013). Six identifiable peaks corresponding to aromatic GSH-CGA, which could be roughly divided into two sets of three peaks based on similar peak areas after integration, shared fragmentation patterns evidencing scission of GSH's cysteinyl C—S bond, yielding a GSH fragment of *m/z* 274.1 Table 3. Other fragments corresponding to fragmentation of GSH, including *m/z* 145.1, 195.0, 393.1, 531.1, and 585.2 were observed, along with an ion with *m/z* 468.1 indicating neutral loss of QA (Xie, Zhong, & Chen, 2013). Each set of three peaks is hypothesized to have been generated by reactions with the 3-, 4- and 5-isomers of CGA, while the two sets of three peaks may differ based on the location of the thioester bond, which likely forms predominantly at the 2′ position of the quinone ring followed by the 5′ position.

Total abundances of the aromatic GSH-CGA conjugates exhibited temporal trends that differed by pH. At pH 8.0, the aromatic conjugates appeared to increase during the first 4 hr of incubation with no significant increase observed by 24 hr, which was then followed by a significant increase of approximately five times by 48 hr. At pH 9.0, abundances were greater than those at pH 8.0 for the first 8 hr with no significant changes, suggesting rapid formation during the first minutes of the reaction. Abundances increased by 24 hr and then decreased by 48 hr, suggesting further reactions that eventually consumed some of the aromatic conjugates at elevated pH over long durations.

Three dominant benzylic GSH-CGA peaks with *m/z* of 662.2 were observed, identified by fragmentation of the thioether C—S bond yielding GSH and CGA fragments with *m/z* 308.1 and 355.1, respectively, along with fragments corresponding of *m/z* 179.1, 233.1, 533.2, and 587.2 indicative of fragmentation of GSH in line with patterns reported by Xie et al. (2013) (Fig. 4C and S5B). The three primary peaks were again hypothesized to arise from isomeric CGA reactants. At least three other *m/z* 662.2 peaks were observed with abundances approximately 100 times less than the three primary peaks were observed, which may arise from the formation of *cis*-CGA isomers or from thiol addition at the 8′ position of CGA.

All benzylic GSH-CGA abundance changes over time exhibited similar trends. The *m/z* 662.2 conjugates increased in concentration during the first 8 hr at pH 8.0 and during the first 4 hr at pH 9.0. Abundances remained nearly constant at pH 8.0 but decreased over time at pH 9.0.

Mono-glutathionyl conjugates were also observed to form diglutathionyl-CGA conjugates after two and 12 hr in GSH-containing solutions at pH 8.0 and 9.0, respectively. The MS^2 spectra for these

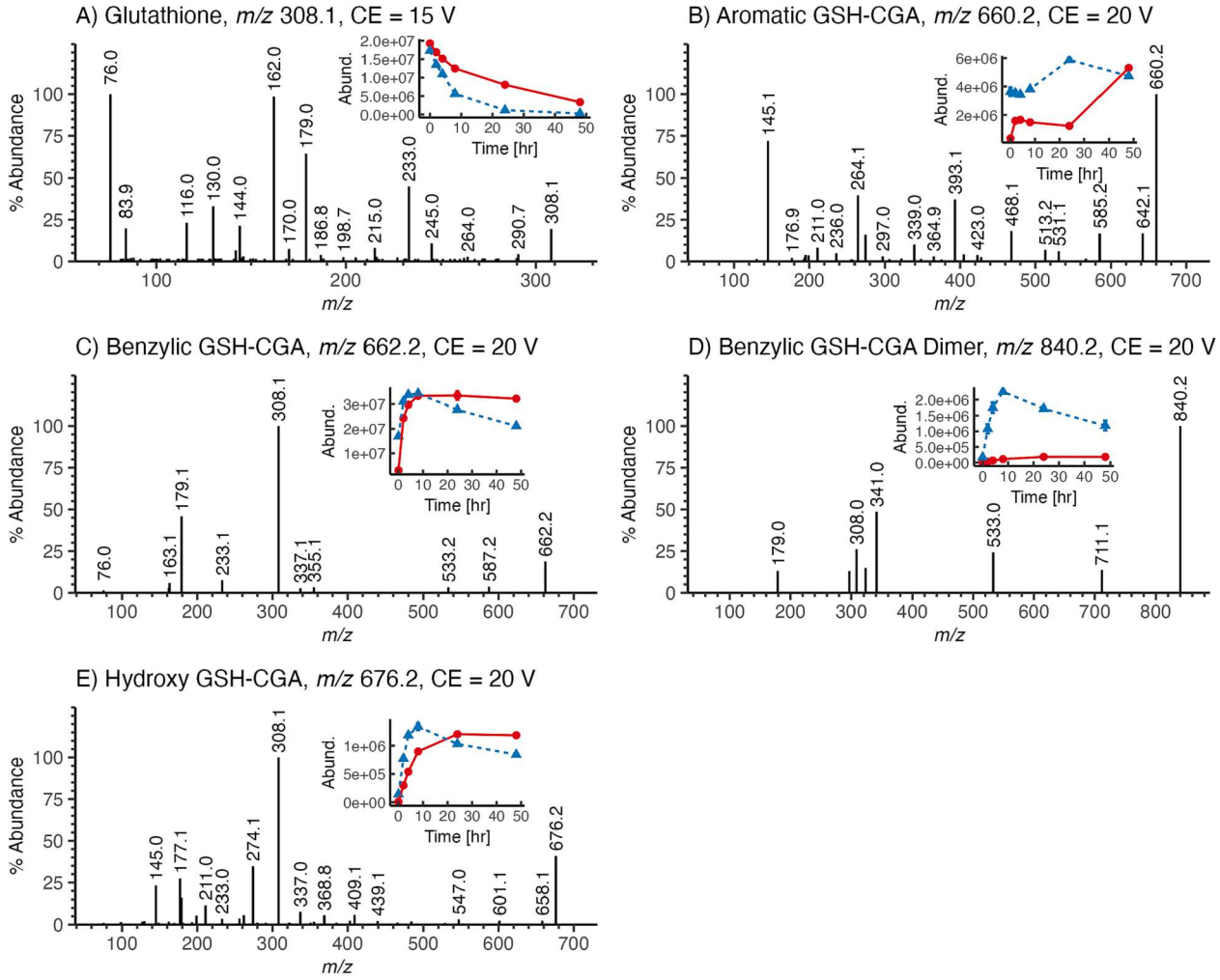

Fig. 4. Fragmentation of conjugates identified in chlorogenic acid-lysine-glutathione solutions. Inset plots illustrate abundance changes over the 48 hr reaction duration, where the solid red line (—●—) describes solutions at pH 8 and the blue dashed line (- -▲- -) describes solutions at pH 9. (For interpretation of the references to color in this figure legend, the reader is referred to the web version of this article.)

Table 3
Precursor ions, fragments, and tentative identifications of compounds observed in chlorogenic acid-lysine-glutathione (GSH) solutions.

Precursor	Tentative Identification	Voltage	Fragments
308	Glutathione	15	308.1 (19), 245.0 (11), 233.0 (45), 215.0 (8), 179.0 (64), 170.0 (7), 162.0 (99), 144.0 (21), 130.0 (33), 116.0 (23), 83.9 (20), 76.0 (100)
488	Aromatic GSH-CA	15	488.2 (7), 308.1 (82), 233.1 (21), 181.1 (8), 179.1 (100), 162.0 (9)
490	Benzylic GSH-CA	15	490.2 (10), 361.1 (5), 310.1 (87), 309.1 (16), 308.1 (16), 235.1 (18), 233.0 (7), 181.0 (100), 180.0 (21), 179.0 (37), 164.0 (7)
613	Glutathione disulfide	15	613.3 (100), 595.2 (16), 538.1 (8), 484.2 (54), 409.1 (9), 355.1 (72), 231.0 (7)
646	Dehydroxy GSH-CGA	15	646.2 (100), 571.1 (6), 517.0 (12), 339.2 (5), 308.1 (59), 179.0 (19), 147.0 (12)
660	Aromatic GSH-CGA	20	660.2 (100), 642.1 (17), 585.2 (17), 531.1 (6), 513.2 (7), 468.1 (18), 393.1 (37), 339.0 (10), 274.1 (16), 264.1 (40), 211.0 (8), 145.1 (72)
662	Benzylic GSH-CGA	20	662.2 (19), 308.1 (100), 233.1 (7), 179.1 (46), 163.1 (6)
676	Hydroxy GSH-CGA	20	676.2 (41), 409.1 (6), 368.8 (6), 337.0 (8), 308.1 (100), 274.1 (35), 261.9 (6), 211.0 (12), 198.9 (5), 179.0 (16), 177.1 (27), 145.0 (23)
840	Benzylic GSH-CGA Dimer	20	840.2 (100), 711.1 (14), 533.0 (24), 341.0 (49), 322.9 (15), 308.0 (26), 297.0 (13), 179.0 (13)

CA refers to caffeic acid.

compounds with *m/z* 967.3 typically included a peak at 838.2 a peak at 838.2, corresponding to loss of a pyroglutamic acid fragment from one of the GSH moieties, and a peak at 660.2, indicating loss of the benzylic GSH moiety to yield an aromatic GSH-CGA conjugate. Solutions at pH 9.0 also contained significant coeluting peaks with *m/z* 793.2, corresponding to a diglutathionyl-CA species arising from hydrolysis of the CGA ester bond. Both *m/z* 967.3 and 793.2 consistently coeluted with peaks of 484.2 and 397.2 as doubly-charged species after ionization.

Losses of GSH-CGA conjugates were also attributed to alkaline hydrolysis, yielding aromatic GSH-CA compounds with *m/z* 486.2 and benzylic GSH-CA compounds with *m/z* 488.2 and, which occurred throughout the entire incubation at pH 9.0 but only significantly after 24 hr at pH 8.0.

Several benzylic GSH-CGA dimer compounds with *m/z* 840.2 were also observed, all of which exhibited fragments 533.0, 341.0, 323.1, and 308.0, indicating fragmentation of the benzylic thioester bond and characteristic CGA dimer fragmentation (Fig. 4D and S5D). At pH 9.0, abundances of these compounds increased for the first 8 hr, after which point hydrolysis of the remaining CGA ester bond yielded compounds with *m/z* 666.2. Formation of *m/z* 840.2 compounds remained negligible at pH 8.0, with no significant formation of compounds with *m/z* 666.2. Considering the net consumption of CGA in GSH-containing solutions over the 48 hr incubation was greater than for other samples (Fig. S6), it is hypothesized that specifically the benzylic GSH-CGA conjugates continued to react with CGA molecules after formation. Such behavior may provide another avenue by which color-generating reactions associated with CGA oxidation are mitigated by GSH. Compounds with *m/z* 838.1 and 842.3 may also arise from reactions of GSH-CGA conjugates, though their fragmentation patterns at the collision energies utilized only evidence the presence of GSH in these compounds' structures.

Significant peaks with *m/z* 646.2, exhibiting fragments with *m/z* 308.1, along with a benzylic GSH-CGA-type precursor with *m/z* 339.1, is hypothesized to arise from a dehydroxy-CGA molecule, in addition to a fragment with *m/z* 147.0 that would be generated from loss of a QA moiety. All other peaks in the MS^2 spectra could be attributed to GSH fragmentation. The mechanism by which this dehydroxylated compound would be generated is currently unclear, and thus the identification should be considered tentatively. The presence of fragments of 646.2 within the MS^2 spectra of *m/z* 838.1 compounds suggests these species may be GSH conjugates of a caffeic aldehyde compound arising from in-source fragmentation.

Tentatively identified hydroxylated GSH-CGA conjugates were also observed with *m/z* values of 676.2. Differing fragmentation patterns within the MS^2 spectra of the *m/z* 676.2 peaks may be indicative of both aromatic and benzylic conjugates (Fig. S5C). Peaks at retention times of 1.26, 1.42, 2.17, and 3.22 min did not include fragments of 308.1, while those at 1.84, 2.53, and 2.81 did, potentially indicating the former group consists of aromatic conjugates and the latter consists of benzylic conjugates. The presence of a peak with *m/z* 369.1 in the benzylic conjugates group may be associated with a hydroxylated CGA fragment during benzylic fragmentation, which was commonly observed with a base peak of 177.1, arising from loss of QA. However, all peaks contain fragments of *m/z* 274.1, which can be attributed to a GSH fragment after scission of the cysteinyl C—S bond, and which theoretically occurs significantly for aromatic conjugates (Xie et al., 2013).

4. Limitations

In-source fragmentation of analytes, predominantly of QA moieties of CGA, may influence observed abundances of CGA and its conjugates. Furthermore, Cys and many of its reaction products were poorly retained on the C18 column, likely resulting in significant coelution of these compounds, obscuring the enumeration of isomeric compounds. Future work may instead utilize polar-functionalized or HILIC columns for more effective separation of these compounds.

Analytes described in this work were not synthesized individually, precluding their quantification for kinetic analyses. Similarly, no authentic standards of thiolyl-CGA or thiolyl-CA conjugates are commercially available for comparison of retention times and fragmentation patterns. Future work may leverage existing synthetic and purification techniques for CGA conjugates, such as periodate oxidation of CGA followed by reaction with Cys to yield 2′-Cys-CGA as performed by Poojary et al. (2023). However, the authors reported no formation of the 5′- or 6′-Cys-CGA isomers under reaction conditions, nor was CGA isomerization reported (Poojary, Hellwig, Henle, & Lund, 2023). Modifications to the existing synthesis may be explored to determine the regiospecificity of thiol conjugate reactions.

The reaction conditions in this work are limited to those processed at alkaline conditions or that are exposed to elevated temperatures. While species reported in this work may be relevant to applications such as the alkaline processing of sunflower proteins, which may be improved by the inclusion of Cys or GSH as a means of mitigating color prevention (Pepra-Ameyaw, Lo Verde, Drucker, Owens, & Senger, 2023) or in alkaline formulated beverages containing CGA and proteinaceous ingredients. Other processing conditions may result in significantly different generation of conjugate species. Alkaline processed foods without CGA would not be prone to any green pigment formation due to the complete absence of CGA, such as during soy protein isolation. Future work may benefit from analyzing the presented reactions under acidic conditions or elevated temperatures, which may be expected to limit the degree of conjugate formation or enhance degradative reactions that could enhance brown color development.

5. Conclusion

Investigation of thiolyl-CGA conjugates in the context of food science remains largely relegated to aromatic conjugates, though this work conclusively evidenced the formation of benzylic conjugates and other reaction products in alkaline solutions. As such, continued research on

the complex interactions CGA has with thiols and other compounds under alkaline conditions should continue to be a focus of study, particularly in determining whether these compounds have varied effects on antioxidant activity. Further structural analyses may also more conclusively characterize hydroxylated CGA compounds, which may be of particular interest during alkaline processing of CGA-rich foods.

CRediT authorship contribution statement

Charles T. Drucker: Investigation, Methodology, Writing – original draft. **Amanda R. Cicali:** Investigation. **Andrew M.P. Roberts:** Investigation. **Christine A. Hughey:** Investigation, Methodology, Writing – review & editing. **Lilian Were Senger:** Conceptualization, Supervision, Writing – review & editing.

Declaration of Competing Interest

The authors declare that they have no known competing financial interests or personal relationships that could have appeared to influence the work reported in this paper.

Data availability

in supplement and https://data.mendeley.com/datasets/2s2yvb39nm

Acknowledgments

We thank Chapman University for supporting this work through the Graduate Research Assistantship. This work was also supported by the National Science Foundation Grant CHE-2150091.

Appendix A. Supplementary data

Supplementary data to this article can be found online at https://doi.org/10.1016/j.foodchem.2023.136267 and https://data.mendeley.com/datasets/2s2yvb39nm.

References

Alfieri, M. L., Cariola, A., Panzella, L., Napolitano, A., d'Ischia, M., Valgimigli, L., & Crescenzi, O. (2022). Disentangling the puzzling regiochemistry of thiol addition to o-quinones. *The Journal of Organic Chemistry, 87*(7), 4580–4589. https://doi.org/10.1021/acs.joc.1c02911

Bongartz, V., Brandt, L., Gehrmann, M. L., Zimmermann, B. F., Schulze-Kaysers, N., & Schieber, A. (2016). Evidence for the formation of benzacridine derivatives in alkaline-treated sunflower meal and model solutions. *Molecules, 21*(1), 9. https://doi.org/10.3390/molecules21010091

Claudino, M., Johansson, M., & Jonsson, M. (2010). Thiol–ene coupling of 1,2-disubstituted alkene monomers: The kinetic effect of cis/trans-isomer structures. *European Polymer Journal, 46*(12), 2321–2332. https://doi.org/10.1016/j.eurpolymj.2010.10.001

Drucker, C. T., Senger, L. W., & Pacioles, C. T. (2023). Application of the weibull model to describe the kinetic behaviors of thiol decolorizers in chlorogenic acid-lysine solutions. *Journal of Food Engineering, 339*, Article 111287. https://doi.org/10.1016/j.jfoodeng.2022.111287

Dénès, F., Pichowicz, M., Povie, G., & Renaud, P. (2014). Thiyl Radicals in Organic Synthesis. *Chemical Reviews, 114*(5), 2587–2693. https://doi.org/10.1021/cr400441m

Gigl, M., Frank, O., Irmer, L., & Hofmann, T. (2022). Identification and quantitation of reaction products from chlorogenic acid, caffeic acid, and their thermal degradation products with odor-active thiols in coffee beverages. *Journal of Agricultural and Food Chemistry, 70*(17), 5427–5437. https://doi.org/10.1021/acs.jafc.2c01378

Iacomino, M., Weber, F., Gleichenhagen, M., Pistorio, V., Panzella, L., Pizzo, E., … Napolitano, A. (2017). Stable benzacridine pigments by oxidative coupling of chlorogenic acid with amino acids and proteins: Toward natural product-based green food coloring. *Journal of Agricultural and Food Chemistry, 65*(31), 6519–6528. https://doi.org/10.1021/acs.jafc.7b00999

Ishii, A., Pacioles, C., & Were, L. (2021). Color and structural modifications of alkaline extracted sunflower protein concentrates and isolates using L-cysteine and glutathione. *Food Research International, 147*. https://doi.org/10.1016/j.foodres.2021.110574

Ito, S., Sugumaran, M., & Wakamatsu, K. (2020). Chemical reactivities of ortho-quinones produced in living organisms: Fate of quinonoid products formed by tyrosinase and phenoloxidase action on phenols and catechols. *International Journal of Molecular Sciences, 21*(17). https://doi.org/10.3390/ijms21176080

Kishida, R., Ito, S., Sugumaran, M., Arevalo, R. L., Nakanishi, H., & Kasai, H. (2021). Density functional theory-based calculation shed new light on the bizarre addition of cysteine thiol to dopaquinone. *International Journal of Molecular Sciences, 22*(3), 15. https://doi.org/10.3390/ijms22031373

Liang, N., & Kitts, D. D. (2015). Role of chlorogenic acids in controlling oxidative and inflammatory stress conditions. *Nutrients, 8*(1). https://doi.org/10.3390/nu8010016

Liang, Y. D., & Were, L. (2020). Cysteine's effects on chlorogenic acid quinone induced greening and browning: Mechanism and effect on antioxidant reducing capacity. *Food Chemistry, 309*. https://doi.org/10.1016/j.foodchem.2019.125697

Matei, M. F., Jaiswal, R., & Kuhnert, N. (2012). Investigating the chemical changes of chlorogenic acids during coffee brewing: Conjugate addition of water to the olefinic moiety of chlorogenic acids and their quinides. *Journal of Agricultural and Food Chemistry, 60*(49), 12105–12115. https://doi.org/10.1021/jf3028599

Namiki, M., Yabuta, G., Koizumi, Y., & Yano, M. (2001). Development of free radical products during the greening reaction of caffeic acid esters (or chlorogenic acid) and a primary amino compound. *Bioscience Biotechnology and Biochemistry, 65*(10), 2131–2136. https://doi.org/10.1271/bbb.65.2131

Napolitano, A., De Lucia, M., Panzella, L., & d'Ischia, M. (2008). The "benzothiazine" chromophore of pheomelanins: A reassessment. *Photochemistry and Photobiology, 84*(3), 593–599. https://doi.org/10.1111/j.1751-1097.2007.00232.x

Pepra-Ameyaw, N. B., Lo Verde, C., Drucker, C. T., Owens, C. P., & Senger, L. W. (2023). Preventing chlorogenic acid quinone-induced greening in sunflower cookies by chlorogenic acid esterase and thiol-based dough conditioners. *LWT, 174*, Article 114392. https://doi.org/10.1016/j.lwt.2022.114392

Poojary, M. M., Hellwig, M., Henle, T., & Lund, M. N. (2023). Covalent bonding between polyphenols and proteins: Synthesis of caffeic acid-cysteine and chlorogenic acid-cysteine adducts and their quantification in dairy beverages. *Food Chemistry, 403*, Article 134406. https://doi.org/10.1016/j.foodchem.2022.134406

Prigent, S. V. E., Voragen, A. G. J., Li, F., Visser, A. J. W. G., van Koningsveld, G. A., & Gruppen, H. (2008). Covalent interactions between amino acid side chains and oxidation products of caffeoylquinic acid (chlorogenic acid). *Journal of the Science of Food and Agriculture, 88*(10), 1748–1754. https://doi.org/10.1002/jsfa.3275

R Core Team. (2022). *R: A language and environment for statistical computing*. Vienna, Austria: R Foundation for Statistical Computing.

Smith, C. A., Want, E. J., O'Maille, G., Abagyan, R., & Siuzdak, G. (2006). XCMS: Processing mass spectrometry data for metabolite profiling using nonlinear peak alignment, matching, and identification. *Analytical Chemistry, 78*(3), 779–787. https://doi.org/10.1021/ac051437y

Tošović, J., & Marković, S. (2019). Antioxidative activity of chlorogenic acid relative to trolox in aqueous solution – DFT study. *Food Chemistry, 278*, 469–475. https://doi.org/10.1016/j.foodchem.2018.11.070

Tošović, J., Marković, S., Dimitrić Marković, J. M., Mojović, M., & Milenković, D. (2017). Antioxidative mechanisms in chlorogenic acid. *Food Chemistry, 237*, 390–398. https://doi.org/10.1016/j.foodchem.2017.05.080

Wildermuth, S. R., Young, E. E., & Were, L. M. (2016). Chlorogenic acid oxidation and its reaction with sunflower proteins to form green-colored complexes. *Comprehensive Reviews in Food Science and Food Safety, 15*(5), 829–843. https://doi.org/10.1111/1541-4337.12213

Xie, C., Zhong, D., & Chen, X. (2013). A fragmentation-based method for the differentiation of glutathione conjugates by high-resolution mass spectrometry with electrospray ionization. *Analytica Chimica Acta, 788*, 89–98. https://doi.org/10.1016/j.aca.2013.06.022

Yabuta, G., Koizumi, Y., Namiki, K., Hida, M., & Namiki, M. (2001). Structure of green pigment formed by the reaction of caffeic acid esters (or chlorogenic acid) with a primary amino compound. *Bioscience Biotechnology and Biochemistry, 65*(10), 2121–2130. https://doi.org/10.1271/bbb.65.2121